Phytoplankton growth responses to Asian dust additions in the Northwest Pacific Ocean versus the Yellow Sea

Chao Zhang[1], Huiwang Gao[1*], Xiaohong Yao[1], Zongbo Shi[2], Jinhui Shi[1], Yang Yu[1], Ling Meng[1] and Xinyu Guo[3]

[1]Key Laboratory of Marine Environment and Ecology, Ministry of Education of China, Ocean University of China, Qingdao, China

[2]School of Geography, Earth and Environmental Sciences, University of Birmingham, Birmingham, U.K

[3]Center for Marine Environmental Studies, Ehime University, Japan

*Correspondence to: hwgao@ouc.edu.cn

Abstract. In this study, five on-board microcosm experiments were performed in the subtropical gyre, *Kuroshio* Extension region of the Northwest Pacific Ocean (NWPO) and the Yellow Sea (YS), in order to investigate phytoplankton growth following the addition of artificially modified mineral dust (AM-dust) and various nutrients (nitrogen-N, phosphorus-P, iron-Fe, N+P, and N+P+Fe). The two experiments carried out with AM-dust addition in the subtropical gyre showed a maximum chlorophyll *a* (Chl *a*) concentration increase of 1.7- and 2.8-fold, while the cell abundance of large-sized phytoplankton (>5 µm) showed a 1.8- and 3.9-fold increase, respectively, relative to the controls. However, in the *Kuroshio* Extension region and the YS, the increases in maximum Chl *a* and cell abundance of large-sized phytoplankton following AM-dust addition were at most 1.3-fold and 1.7-fold larger than those in the controls, respectively. A net conversion efficiency index (NCEI) newly proposed in this study, size-fractionated Chl *a*, and the abundance of large-sized phytoplankton were analysed to determine which nutrients contribute to support phytoplankton growth. Our results demonstrate that a combination of nutrients, NP or NPFe as well as other micro-constituents, are responsible for phytoplankton growth in the subtropical gyre following AM-dust addition. Single nutrient addition, i.e., N in the *Kuroshio* Extension region and P/N in the YS, controls the phytoplankton growth following AM-dust addition. In the AM-dust-addition experiments, wherein the increased NP or P were identified to determine phytoplankton growth, the dissolved inorganic P from AM-dust (8.6 nmol L^{-1}) was much lower than the theoretically estimated minimum P demand (~20 nmol L^{-1}) for phytoplankton growth. These observations suggest that additional supply augments the bioavailable P stock in incubated seawater with AM-dust addition, most likely due to an enhanced solubility of

P from AM-dust or re-mineralization of the dissolved organic P.

1 Introduction

Aeolian dust deposition can supply bioavailable nutrients such as nitrogen (N), phosphorus (P), and iron (Fe) to the upper ocean layers (Duce et al., 1991; Jickells et al., 2005; Kanakidou et al., 2012). Observational and modelling studies have demonstrated that external nutrient input can stimulate the primary productivity, strengthen the nitrogen fixation, alter the phytoplankton size, and potentially enhance the carbon sequestration by the biological pump in the ocean (Mills et al., 2004; Maranon et al., 2010; Liu et al., 2013). A well-recognized aspect of dust deposition is the iron fertilization effect in high-nutrient low-chlorophyll (HNLC) regions (Martin, 1991; Boyd et al., 2007). Recently, many studies have attempted to explore the primary chemicals that promote phytoplankton growth following dust deposition in low-nutrient low-chlorophyll (LNLC) regions, which cover ~60% of the ocean area worldwide (Moore et al., 2008; Guo et al., 2012; Ridame et al., 2014; Li et al., 2015). For example, dissolved Fe and P from deposited dust were reported to stimulate nitrogen fixation in the oligotrophic region of the eastern tropical North Atlantic Ocean (Mills et al., 2004). In the oligotrophic region of the western North Atlantic Ocean off Barbados, a greater concentration of dissolved N and Fe relative to P, arising from the deposited dust, likely favoured the growth of *Prochlorococcus*, but limited the activity of diazotrophs (Chien et al., 2016). Moreover, the reported positive effect of dust deposition on the primary production in the central Atlantic Ocean decreased with increasing oligotrophy of the seawater (Maranon et al., 2010). However, studies in areas other than the North Atlantic Ocean and the Mediterranean Sea are scarce.

Dust particles frequently mix with anthropogenic aerosols on their transport pathway to the oceans (Guieu et al., 2010; Shi et al., 2012; Herut et al., 2016). The response of phytoplankton to the added dust particles mixed with anthropogenic aerosols appeared to be more sensitive in oligotrophic waters than in moderately nutrient-enriched waters (Guo et al., 2012). Unlike in HNLC and LNLC regions of the oceans, the response of phytoplankton to dust deposition in coastal seas that receive a

relatively large quantity of nutrients from rivers is poorly understood. A few studies showed that dissolved N from the added dust likely stimulated phytoplankton growth in the Yellow Sea (YS) (Liu et al., 2013). Added Fe instead of other dissolved nutrients from atmospheric deposition played an important role in stimulating phytoplankton growth in the Eastern China Sea (Meng et al., 2016). The complex responses of phytoplankton growth to dust deposition are worthy of investigation.

The N:P ratio of dust deposition is much higher than the Redfield ratio (N:P=16) (Baker et al., 2003; Guo et al., 2012), which reflects the average cellular N:P stoichiometry for oceanic phytoplankton (Arrigo, 2005). Although the deposited P was deficient relative to the demands of the resident phytoplankton in the ocean surface, a few studies showed that the input of dust could compensate for P deficiency to some extent by stimulating the biogenic conversion of dissolved organic P (DOP) to dissolved inorganic P (DIP), or a slow release of DIP from dust (Ridame and Guieu, 2002; Mackey et al., 2012; Krom et al., 2016). This supply of bioavailable P seemingly varies substantially across different oceanic regions and is affected by many factors, including dust sources and its mixing with anthropogenic pollutants, P demand, and uptake of nutrients that are co-limiting for phytoplankton in the seawater (Mackey et al., 2012). It remains a challenge to accurately estimate the supply of bioavailable P for phytoplankton growth, induced by dust deposition in specific environments.

The arid regions of eastern Asia are the most important mineral dust source to the western Pacific Ocean (Shao et al., 2011). In spring, strong westerly winds can carry large amounts of mineral dust from Asian continent along a corridor between 25°N to 45°N, and bring significant amounts of nutrients to downwind areas, including the coastal seas of China and Japan, and the Northwest Pacific Ocean (NWPO) (Shao et al., 2011). During this long-range transport, the contents of bioavailable nutrients in the Asian dust might increase through mixing with air pollutants such as sulphur dioxide and nitrogen oxides (Formenti et al., 2011). The subtropical gyre in the NWPO is a LNLC region with $NO_3^-+NO_2^-$ and PO_4^{3-} concentrations generally maintained at nanomolar levels (Hashihama et al., 2009). Seawater in the *Kuroshio* Extension region, however, show flexible characteristics in nutrients, which is ascribed to the confluence of the *Oyashio* current with replete nutrient stocks, and that of the *Kuroshio* current with impoverished nutrient stocks (Measures et al., 2006; Kitajima et al., 2009). On the other hand, the YS is a semi-enclosed continental shelf region, which is located in the margin of the NWPO surrounded by the Chinese

mainland and the Korean Peninsula. Seawater in the YS exhibits high nutrient levels but varying nutrient-limiting conditions, e.g., N or P limitation (Liu et al., 2003). Thus, the NWPO and YS are the ideal zones to explore how Asian dust deposition influences phytoplankton growth and community size shifts under varying nutrient levels in seawaters.

In this study, we conducted on-board bioassay incubations using artificially modified mineral dust (AM-dust) collected from the Gobi Desert of China and native phytoplankton assemblages collected from the NWPO and YS, to investigate the effect of atmospheric nutrients and trace metal inputs on phytoplankton growth. The measured concentrations of Chl a in the nutrient treatments (i.e., N, P, Fe, N+P, and N+P+Fe additions) against the control were used to determine the nutrient limitation in the subtropical gyre, the *Kuroshio* Extension region of the NWPO and the YS, respectively. The concentrations of total and size-fractionated Chl a, as well as the abundances and community structures of large-sized phytoplankton (> 5 μm) were determined to study the responses of different-sized phytoplankton to the nutrients supplied by AM-dust. A net conversion efficiency index (NCEI) is proposed to identify the key nutrient(s) in determining the increase of Chl a concentrations, following AM-dust addition at different incubation stations. Finally, we analysed the minimum P consumption that supports phytoplankton growth following AM-dust addition, to estimate the P budget of the added dust.

2 Materials and Methods

2.1 Preparation of AM-dust

We collected surface soil samples (42.37°N, 112.97°E) from the Gobi Desert, one of the most important sources of dust events crossing over the YS and NWPO (Ooki and Uematsu, 2005; Shao et al., 2011). The soil samples were crushed, sieved to less than 20-μm particle size, and freeze-dried (Shi et al., 2009). To account for the aging of dust particles in the atmosphere, we followed Guieu et al. (2010) by mixing the soil with synthetic cloud water in a cleaned polypropylene bottle, then spread the solution on a polystyrene tray and evaporated the aqueous phase under clean air flow in a fume hood. A more detailed modification protocol is presented in the Supplementary Information (Text S1 & Table S1). These treated soil dust particles are referred to as 'AM-dust'. Clean plastic or plastic-coated materials were used for the preparation of AM-dust to avoid metal contamination.

2.2 Experimental design

100 Five AM-dust addition bioassay experiments were carried out on-board the *R/V Dongfanghong II* during two cruises in 2014 at stations Ar4, G7, and K4 in the NWPO (Cruise I: March–April), and B7 and H10 in the YS (Cruise II: April–May) (Fig. 1 & Table 1). Based on the baseline Chl *a* concentrations (Table 1), the five stations were redefined as S1 (Ar4), S2 (G7), S3 (K4), S4 (B7), and S5 (H10), in the ascending order. Surface seawater (2–5 m) was collected using acid-washed Teflon-coated Go-Flo bottles mounted on a SeaBird CTD assembly (SBE 9/11, USA) and filtered through a 200-μm acid-washed mesh to

105 remove larger grazers. Filtered seawater with nine different additions (true replicates, detailed in Table 2) was randomly dispensed into 18 pre-acid-washed and sample-rinsed (three times) Nalgene polycarbonate bottles (20-L each). Water samples in the incubated bottles were collected before the additions, for characterizing the baseline seawater samples, and immediately after the additions, for characterizing the amended seawater (day 0). Surface seawater was pumped into the microcosm equipment, i.e., three large plastic vessels, to stabilize the temperature of the incubation systems (Liu et al., 2013). The

110 incubation experiments were processed over 9–10 days under natural light. Water samples were collected from incubated bottles at 08:00 am every day except day 1 (i.e., day 2 through day 9/10), for determining Chl *a* and nutrient concentrations, and on certain days for phytoplankton identification and enumeration.

Treatments included AM-dust and single nutrient (N, P, or Fe) additions as well as N+P and N+P+Fe (Table 2). Previous

115 studies showed that annual deposition flux of Asian dust in the YS and NWPO regions ranged from 10 to 80 $g\,m^{-2}\,yr^{-1}$ (Gao et al., 1992; Brown et al., 2005). An extreme dust storm event accompanied by wet precipitation in the YS can lead to a considerable dust deposition flux in this range (Shi et al., 2012). Considering these results, we added 2 mg L^{-1} of the AM-dust to the incubated seawater to simulate deposition due to a strong dust event (20 g m^{-2}) in the upper 10 m water layer in the YS (Liu et al., 2013). We added the same amount of AM-dust for incubation experiments in the NWPO for comparison. This

120 amount of added dust has been widely used in other studies as well (Mills et al., 2004; Maranon et al., 2010). Based on the N-deposition flux in the NWPO (Kim et al., 2014) and an estimate of the N addition by a dust event in the surface water of the

YS (Shi et al., 2012), we added 40 µmol NaNO$_3$ into the 20-L bottles for the N-related treatments (N, N+P, and N+P+Fe additions), to increase the N concentration by 2 µmol L^{-1}. The added P and Fe in incubation systems were 0.2 µmol L^{-1} and 2 nmol L^{-1}, respectively, based on the nutrient-addition experiments conducted in the NWPO and YS (Noiri et al., 2005; Liu et al., 2013) (Table 2).

One-way analysis of variance (ANOVA) was used to assess significant differences in the mean values of the selected parameters among various treatments, and then Dunnett's test was used to compare these treatments with the control using SPSS (Statistical Product and Service Solutions) software.

2.3 Chl *a* concentration

From each bottle, a 300-mL seawater sample was sequentially filtered through 20-, 2-, and 0.2-µm Whatman polycarbonate filters to determine size-fractionated Chl *a* concentrations, i.e., pico- (0.2–2 µm), nano- (2–20 µm), and micro-sized (> 20 µm) Chl *a*. The pigments on the filters were extracted in 90% acetone at -20 °C over 24h in the dark, and measured on a Turner Designs Trilogy fluorometer (Strickland and Parsons, 1972). The total Chl *a* concentration was calculated as the sum of the three size-fractionated values.

2.4 Inorganic nutrients and trace metals

To determine the soluble nutrients such as NO_3^-, NO_2^-, NH_4^+, and PO_4^{3-} leached from AM-dust, oligotrophic seawater was pre-filtered by 0.2 µm glass fiber filters and used for extracting these ions at ~0°C for 30 minutes in an ultrasonic bath filled with ice and water. A 200-mL seawater sample retrieved from each of the incubation bottles was filtered through pre-acid-washed cellulose acetate membranes and filtrates were stored immediately at -20 °C in acid-washed high-density polyethylene bottles for nutrients analysis in the laboratory. Soluble nutrients leached from AM-dust and in the incubated seawaters were measured following the automated colorimetric technique described by Grasshoff et al. (1999) and Ridame et al. (2014), using a QuAAtro

Continuous Flow Analyzer (SEAL Analytical). Detection limits of this instrument were defined as three times the standard deviation of the blank, which corresponds to 30 nM, 7 nM, 80 nM, and 40 nM for NO_3^-, NO_2^-, NH_4^+, and PO_4^{3-}, respectively. Note that the NH_4^+ concentrations were determined only for the leached solution of AM-dust. We followed the method proposed by Hsu et al. (2010) to determine the concentrations of soluble trace metals leached from AM-dust using an ICP-MS. The recovery yield, accuracy, and detection limit are summarized in Table S2.

2.5 Phytoplankton identification and enumeration

Seawater samples (300-mL volume) were collected from the baseline seawaters at each station and incubated bottles on day 4 from S1 and S2, day 3 from S3 and S5, and day 5 from S4 for the identification and enumeration of large-sized phytoplankton (> 5 µm). The sampling dates selected during the incubation experiment were either close to or corresponded exactly with the days that showed the maximum Chl *a* concentrations (Figure S1). The sampled seawater was fixed with 1% Lugol's iodine and stored in dark until microscopic observation in the laboratory (Burson et al., 2016). Before analysis, the preserved samples were settled for 48 h in the dark and then concentrated to 10-mL volume in glass cylinders. Large-sized phytoplankton was identified and enumerated using a Nikon ECLIPSE TE2000-U inverted microscope. To illustrate the responses of different phytoplankton to various additions, the detected phytoplankton species were divided into two major functional groups: diatoms and dinoflagellates. The dominant species of diatoms found in this study were *Nitzschia* spp., *Chaetoceros* spp., *Thalassiosira* spp., *Skeletonema* spp., *Cylindrotheca closterium*, and *Rhizosolenia setigera*.

2.6 Protocol of data analysis

In this study, Chl *a* concentrations generally showed a bell-shape growth curve at all stations with the maximum concentration occurring around 2–5 days (Fig. S1). We focused on analysing the initial 2–5 days, which showed a successive increase in the incubation period. The duration of 2–5 days for incubation has been widely used in other microcosm experiments (Herut et al., 2005; Tanaka et al., 2011; Guo et al., 2012; Li et al., 2015) and is supposed to minimize the effects of bottle enclosure and a

possible deviation from the natural environment (Mackey et al., 2012; Coelho et al., 2013).

170   A net conversion efficiency index (NCEI) was introduced to quantify the differences in N utilization efficiency among the AM-dust treatments and N, N+P, and N+P+Fe treatments. NCEI (unit: $\frac{\mu g\ L^{-1}}{\mu mol\ L^{-1}}$, i.e., $g\ mol^{-1}$) was calculated using the following equation:

$$NCEI = \frac{\sum_{i=0}^{t}(Chl\ a_{Ti} - Chl\ a_{Ci})}{\Delta N} \tag{1}$$

where Chl a_{Ti} and Chl a_{Ci} represent the Chl a concentrations on the ith day, i.e., day 0, day 2–day 3/5, in the treatments and the

175   control (µg L^{-1}), respectively. ΔN is the decreased N concentration in the treatment minus that in the control during the successive increase in the incubation period (µmol L^{-1}). The decreased N concentration equals to the difference in $NO_3^- + NO_2^-$ before and after the initial increase period. A large NCEI value represents a positive effect of the added N on phytoplankton growth, and a value close to zero represents no effect. Larger the NCEI value, higher is the N utilization efficiency by the phytoplankton. Theoretically, the maximum increase of Chl a in concentration can also be used to calculate NCEI. Considered

180   the accumulation and degradation of Chl a, the real net conversion efficiency should be among the NCEI values between the two approaches.

We also defined the consumed ratio of N:P (hereafter, $C_{N:P}$) and supply ratio of N:P (hereafter, $S_{N:P}$) to illustrate the changing stocks of bioavailable N and P in various incubation experiments: $C_{N:P}$ was the ratio of the difference in $NO_3^- + NO_2^-$

185   concentrations at the beginning and the end of the successive increase in incubation period to that of PO_4^{3-}; $S_{N:P}$ was the amended ratio of $NO_3^- + NO_2^-$ to PO_4^{3-} concentrations in the incubated seawaters on day 0 in various treatments.

3 Results

3.1 Characteristics of baseline surface seawater and AM-dust

190   Stations S1, S2, and S3 are in the open ocean and were characterized by warm surface seawaters with Sea Surface Temperature

(SST) larger than 18°C, and deep mixed layer with a depth larger than 80 m. On the other hand, stations S4 and S5 are in the YS and the SST and MLD therein were less than 13°C and 20 m, respectively (Table 3). The winter cooling induces a lower water temperature in the shallow YS than in the deep open ocean. Therefore, the short warming time before our observations during the springtime cannot reverse this situation. The weaker winds as well as lesser loss of heat flux over the land-surrounding YS than over the open ocean lead to the shallower mixed depth at S4 and S5 than at S1-S3.

Low concentrations of Chl a ($\leqslant$ 0.50 μg L^{-1}) and nutrients (NO$_3^-$+NO$_2^-$ $\leqslant$ 0.26 μmol L^{-1}, PO$_4^{3-}$ = 0.05 μmol L^{-1}) were observed at S1 and S2 in the subtropical gyre of the NWPO (Table 1), indicating oligotrophy (Hashihama et al., 2009). At S3 in the *Kuroshio* extension and S4 in the YS, Chl a and nutrient concentrations were at least 2-fold higher than those at S1 and S2, indicating an increased trophic state at S3 and S4. Although the nutrient levels at S5 in the YS were comparable to those at S1, the Chl a concentration of 2.74 μg L^{-1} was close to the values during spring blooms in the YS (Liu et al., 2003; Fu et al., 2009; Liu et al., 2013). The N:P ratios at S1, S2, S3, and S5 were far lower than the Redfield Ratio (16:1), while that at S4 was as high as 32 (Table 2). Pico-sized Chl a accounted for >70% of the total Chl a at S1 and S2, but it decreased to less than ~50% at S3, S4, and S5. Specifically, large-sized phytoplankton abundance showed an increasing trend from < 20 cells mL^{-1} at S1 and S2 to 35 cells mL^{-1} at S4 and 79 cells mL^{-1} at S3, and to the highest value of 314 cells mL^{-1} at S5. Diatoms dominated the large-sized phytoplankton community at S1, S3, and S5, and a codominance of dinoflagellates was noted at S2 and S4 (Table 1).

The concentration of dissolved inorganic nitrogen (DIN, i.e. NO$_3^-$+NO$_2^-$+NH$_4^+$) in the AM-dust was 577 μmol g^{-1} (Table 3) and increased by a factor of four against that in the untreated dust. A notable increase in the PO$_4^{3-}$ content (4.3 μmol g^{-1}) in the AM-dust was observed, relative to the untreated dust (1.3 μmol g^{-1}). The abundances of DIN, PO$_4^{3-}$, and soluble Fe in the AM-dust were generally consistent with the values observed in a strong dust event that occurred over the YS in the spring of 2007 (Shi et al., 2012). The N:P ratio of ~134 in the AM-dust was far greater than 16 (Redfield Ratio), and similar to those in Asian dust aerosols previously reported (Shi et al., 2012; Liu et al., 2013; Chien et al., 2016). The NO$_3^-$+NO$_2^-$ concentration in the incubated seawater after AM-dust addition increased up to ~1.13 μmol L^{-1} (Table 3 & Fig. 2), larger than the baseline NO$_3^-$

+NO$_2^-$ stocks at S1, S2, S3, and S5, but accounted only for approximately 1/3rd of the baseline stock at S4 (Table 2). However, the increase in PO$_4^{3-}$ (~8.6 nmol/L) following AM-dust additions was negligible, compared with the baseline P stock at each station (Tables 2 & 3).

3.2 Variation in nutrient and total Chl *a* concentrations during incubation experiments

220 During the successive increase in the incubation period (initial 2–5 days of the incubations, Sect. 2.6), NO$_3^-$+NO$_2^-$ and PO$_4^{3-}$ concentrations generally showed a decline in the control and all treatments (Fig. 2). At each station, the most obvious decline of NO$_3^-$+NO$_2^-$ and PO$_4^{3-}$ in concentration in various treatments occurred when N+P or N+P+Fe was added together. The net declines were 1.49~4.66 µmol L^{-1} for NO$_3^-$+NO$_2^-$ and 0.18~0.27 µmol L^{-1} for PO$_4^{3-}$. The decline was 0.49~2.99 µmol L^{-1} for NO$_3^-$+NO$_2^-$ and 0.10~0.27 µmol L^{-1} for PO$_4^{3-}$ followed by N and P additions, respectively. For P addition alone at S4, the decline

225 of PO$_4^{3-}$ was comparable to those in combined nutrient additions (0.27 µmol L^{-1}) and that of NO$_3^-$+NO$_2^-$ (2.99 µmol L^{-1}) was 1.3-fold larger relative to the control. Correspondingly, addition of N+P+Fe induced the largest increases in total Chl *a* (hereafter, Chl *a*) among all treatments, and the increases were significant against the controls (Fig. 3, $p < 0.05$) at all stations (Fig. 3). The maximum concentrations of Chl *a* in the N+P+Fe treatments reached 1.70 µg L^{-1} at S1 (day 4), 1.65 µg L^{-1} at S2 (day 5), 3.50 µg L^{-1} at S3 (day 3), 4.98 µg L^{-1} at S4 (day 4), and 5.08 µg L^{-1} at S5 (day 2), respectively. This was a 1.9- to 7.1-

230 fold increase compared to the baseline and was 1.5- to 3.0-fold larger than the controls in the five incubation experiments. The time-series of Chl *a* in N+P and N+P+Fe treatments almost overlapped at all stations except S2, where the maximum value of Chl *a* in the N+P treatment (1.15 µg L^{-1}) was only 70% of that in the N+P+Fe treatment. Significant increases in Chl *a* relative to the control were also observed in N treatments at S1, S2, S3, and S5, and in P treatments at S2 and S4 ($p < 0.05$). The maximum concentrations of Chl *a* in the N treatments at S1 (0.73 µg L^{-1} on day 3), S2 (0.67 µg L^{-1} on day 2), S3 (2.14 µg L^{-1}

235 on day 3), S5 (4.34 µg L^{-1} on day 2), and in the P treatments at S2 (0.79 µg L^{-1} on day 2) and S4 (4.46 µg L^{-1} on day 3) showed a 1.3- to 3.1-fold increase compared to the baseline and were 1.2- to 1.6-fold larger than the controls. There was no significant increase in Chl *a* relative to the control in the rest of the additions at the five stations.

Followed the addition of AM-dust, NO$_3^-$+NO$_2^-$ concentrations declined by 1.06 µmol L^{-1} at S1, 0.88 µmol L^{-1} at S2, 1.36 µmol

L^{-1} at S3, 2.93 μmol L^{-1} at S4, and 0.36 μmol L^{-1} at S5, respectively. The declines were generally larger than the values in the baseline (Fig. 2). PO$_4^{3-}$ concentrations in AM-dust treatments declined by 0.04-0.11 μmol L^{-1} and were similar to those of the control during the successive increase in the incubation period at each station. Correspondingly, the maximum concentration of Chl *a* following AM-dust addition was 1.04 μg L^{-1} at S1 (day 5), 1.54 μg L^{-1} at S2 (day 5), 2.23 μg L^{-1} at S3 (day 2), 3.27 μg L^{-1} at S4 (day 5), and 3.13 μg L^{-1} at S5 (day 2), respectively (Fig. 3), which was 1.1- to 4.4-fold larger against the baseline. The increases in Chl *a* were significant different ($p < 0.05$) from the control at S1, S2, S3, and S5. The maximum Chl *a* concentration following AM-dust addition was 1.7-fold, 2.8-fold, and 1.3-fold of those in the controls at S1, S2, and S3, respectively. At S4 and S5, the maximum Chl *a* concentration in the AM-dust treatments was comparable to those in the controls. However, the Chl *a* concentrations remained relatively high in the AM-dust treatments, while showing a decreasing trend in the controls (Fig. 3).

3.3 Variation in the size-fractionated Chl *a* concentrations during incubation experiments

When the size-fractionated Chl *a* was examined in various treatments at the five stations, a few notable changes were observed, as highlighted below.

a) In the controls, the dominant contributors to the total Chl *a* were pico-sized cells at S1, S2, S4, and nano-sized cells at S5, while they changed from pico-sized to micro-sized cells at S3 during the successive increase in the incubation period (Fig. 4). Addition of AM-dust increased the Chl *a* concentrations of all sizes and the dominant contributor was consistent with those in the controls at the five stations. However, the magnitude of Chl *a* increase was the highest for micro- or nano-sized cells following AM-dust additions. For example, the largest increase in maximum Chl *a* occurred in micro-sized cells at S1 (2.0-fold), S2 (4.4-fold), S4 (1.4-fold), and S5 (1.6-fold), and in nano-sized cells at S3 (1-3 fold), compared with the controls.

b) Size-fractionated Chl *a* in N+P and N+P+Fe additions showed the largest and similar increases at S1, S3, S4, and S5, especially in the micro-sized range, where the maximum Chl *a* concentrations showed a 1.2- to 6.5-fold increase against the controls (Fig. 4). For station S2, the micro- and nano- sized Chl *a* showed higher increases in N+P+Fe treatments than in N+P treatments, whereas the inverse was true for the pico-sized Chl *a*. Addition of N or P alone also led to an increase in size-

fractionated Chl *a* to some extents at all stations. The size-fractionated Chl *a* in N treatments at S1, S3, and S5 increased

265 noticeably, e.g., the maximum Chl *a* showed the largest increase in nano-sized cells by a factor of 1.6 at S1, and 1.4 at S3, and

in micro-sized cells by a factor of 2.2 at S5, relative to the controls. A clear increase was also observed in the P treatment at

S2 and S4, e.g., the maximum Chl *a* concentrations showed a 1.8-fold (Nano-) and 1.5-fold (Micro-) increase against the

controls (Fig. 4). There was no noticeable increase in any of the size-fractionated Chl *a* following Fe addition at S2 and S4.

c) The results of size-fractionated Chl *a* demonstrated that the micro- and nano-sized phytoplankton generally showed a

270 stronger response than pico-sized cells following AM-dust and various nutrient additions, although the extent of increase varied

among the stations.

3.4 Variation in large-sized phytoplankton abundance and community during incubation experiments

After 2–5 incubation days, diatoms generally dominated the large-sized phytoplankton community in all treatments at the five

275 stations. *Chaetoceros* spp. and *Nitzschia* spp. comprised the largest fraction of diatoms in all treatments at S1, S2, and S3. For

stations S4 and S5, the dominant species of diatoms did not change compared with those in the baseline seawaters (Fig. 5).

Specifically, the cell abundance of large-sized phytoplankton in the controls increased to 37 cells mL^{-1} at S1, 39 cells mL^{-1} at

S2, 422 cells mL^{-1} at S3, 93 cells mL^{-1} at S4, and 643 cells mL^{-1} at S5. Similar to the response of Chl *a*, additions of N+P and

N+P+Fe increased the phytoplankton abundances noticeably in all treatments by about 2.5- to 2.7-fold at S1 and S5, 3.1- to

280 3.3-fold at S3, and 2.7-fold at S4, relative to the controls. For single-nutrient treatments, N additions at S1, S3, and S5, and P

additions at S4 induced the highest increases in cell abundance, with 1.5-, 1.6-, 2.3-, and 1.9-fold higher values, respectively,

than those in the controls. The cell abundance of large-sized phytoplankton in AM-dust treatments relative to the controls

increased by 1.8-fold at S1 and 1.7-fold at S3 and S5, but showed a negligible increase at S4. Moreover, the increases following

AM-dust additions were comparable, and sometimes even larger, relative to those in the N treatments at S1, S3, and S4, but

285 lower than the latter at S5. At S2, the cell abundance with AM-dust addition increased by 3.9-fold against the controls, which

was comparable to those in the N+P treatments (Fig. 5).

4 Discussion

4.1 Nutrient limitation in the NWPO and YS

Building on the results mentioned above (Fig. 2 and Table 2), we summarized the nutrient limiting status at the five stations.

At S1, phytoplankton growth was very likely co-limited by N and P, because: 1) N addition induced significant increase in Chl *a* against the controls ($p < 0.05$), 2) there were significant increases in Chl *a* following N+P additions, compared with the N treatments ($p < 0.05$), and 3) there were no significant differences in Chl *a* between N+P and N+P+Fe treatments ($p > 0.05$). At S2, a significant increase in Chl *a* was observed in the P, N+P, and N+P+Fe treatments ($p < 0.05$) against the controls, and addition of N+P and N+P+Fe induced a significantly larger response, relative to the P treatments ($p < 0.05$). Besides, Chl *a* concentrations in the N+P+Fe treatments were significantly larger than in the N+P treatments on days 4–5. Therefore, we concluded that phytoplankton at S2 were primarily co-limited by N, P, and Fe (Fig. 2). At S3, N addition induced a significant increase in Chl *a* compared with the controls, while an even larger significant increase was observed upon N+P (+Fe) addition, relative to the N treatments. Thus, phytoplankton was primarily co-limited by N and P at S3. Accordingly, $NO_3^-+NO_2^-$ and PO_4^{3-} concentrations in N+P (+Fe) treatments at the three stations decreased by 73%–100%, larger than the decline in $NO_3^-+NO_2^-$ concentrations after adding N alone, and PO_4^{3-} concentrations after adding P alone (43%–70%) (Fig. 3). Such co-limiting conditions have been widely reported in the oceans, especially in oligotrophic regions such as Eastern Mediterranean Sea (Tanaka et al., 2011) and South China Sea (Guo et al., 2012). Moore et al. (2013) argued that low abundances of N and P in oligotrophic environments are likely to simultaneously reach the limiting levels for phytoplankton growth. Note that phytoplankton at S3 in the *Kuroshio* Extension showed a greater response to N rather than P addition. The intrusion of *Kuroshio–Oyashio* transition water from the north and *Kuroshio* water from the southwest, both carrying macronutrients typically with N:P < 16, likely changed the nutrient stocks of the seawaters at S3 (Whitney, 2011; Guo et al., 2012; Yatsu et al., 2013). A low primary productivity in the *Kuroshio* Extension region during the spring time was also indicated by the low availability of nitrate in the seawater (Nishibe at al., 2015).

Similarly, we also found that P and N were the primary limiting nutrients at S4 and S5, respectively (Fig. 2). This is consistent

with the baseline N:P ratios at S4 (>16) and S5 (<16) (Table 2). In fact, the PO_4^{3-} after adding P alone at S4, and $NO_3^-+NO_2^-$ after adding N alone at S5, decreased by 80% and 100%, respectively, during the successive increase in incubation period (Fig. 3). Complex hydrographic conditions, e.g., various riverine inputs and atmospheric deposition, create a large spatiotemporal variation in nutrient concentrations in the YS (Liu et al., 2003). The riverine input and atmospheric deposition with a high N:P (>16) lead to relatively P-deficient conditions, while the rapid uptake by phytoplankton characterized by a lower N:P (<16) during the bloom period likely accelerates the decline of P concentrations in the surface seawaters (Liu et al., 2003; Arrigo, 2005; Liu et al., 2013). In general, the N:P ratios during the spring time in the coastal waters (near S4) are higher than 16 and lower than 16 in the central waters (near S5) of the YS (Fu et al., 2009). The primary P- or N-limiting conditions in the surface seawaters of the YS have also been widely reported in previous studies (Wang et al., 2003; Liu et al., 2013).

4.2 Positive effects of AM-dust on phytoplankton growth in the NWPO and YS

It was clear from the data that AM-dust addition increased the Chl *a* concentrations and large-sized phytoplankton abundance to varying extents at the five stations (Fig. 2, 4&5). However, the increased concentrations of nutrients (e.g., N, P, and Fe) in AM-dust additions were different from those in various nutrient additions. In this study, the NCEI was proposed to quantitatively compare the utilization of N for the growth of phytoplankton among treatments and infer which nutrients in the AM-dust primarily supported phytoplankton growth.

$NO_3^-+NO_2^-$ was theoretically added in the AM-dust treatments at a concentration of 1.13 µmol L^{-1} (Table 3). However, the increase in $NO_3^-+NO_2^-$ concentration was only 0.59–0.85 µmol L^{-1}, immediately after the addition and mixing steps (i.e. on day 0) at the five stations, which was about 52%–75% of the added $NO_3^-+NO_2^-$. Similar trends were also observed for $NO_3^-+NO_2^-$ and PO_4^{3-} concentrations in the nutrient treatments (Fig. 3). The time interval of adding materials to the incubation bottles and sampling seawater for nutrient measurement was 1-2 hr. Microbial uptake, scavenging by cell surface and bottle wall, etc., possibly decreased the concentrations of nutrients at the 1-2 hr, leading to the measured values smaller than the theoretical values. When the concentrations of $NO_3^-+NO_2^-$ and PO_4^{3-} decreased in the seawater, those absorbed by cell surface

and bottle wall had the potential to be released into the solution again for reaching equilibrium (Liu et al., 2013). Thus, the theoretically added N and P, plus the baseline concentrations in the seawaters, were considered the amended concentrations on day 0, which were used for calculating the NCEI.

The added N in AM-dust and N-related treatments generally stimulated phytoplankton growth to varying extents, as indicated by the large NCEI values (Fig. 6). Note that the NCEI in N treatments (hereafter $NCEI_N$) at S4 was around 0 g mol^{-1}, because the phytoplankton was primarily limited by P. Besides, the significant difference in NCEI among various nutrient treatments can also reflect the roles played by other nutrients such as P and Fe in affecting the N utilization efficiency. The NCEI in the N+P+Fe treatments were 1.6 ± 0.1 g mol^{-1} at S1, 1.5 ± 0.1 g mol^{-1} at S3, 2.7 ± 0.2 g mol^{-1} at S4, and 1.4 ± 0.1 g mol^{-1} at S5, comparable with those in N+P treatments (Fig. 6). This suggested that the effect of added Fe on the N-utilization efficiency was negligible at the four stations. Although the added Fe alone had no obvious influence on the Chl a concentration at S2 (Fig. 2), the higher value of $NCEI_{N+P+Fe}$ (1.8 ± 0.0 g mol^{-1}) than the $NCEI_{N+P}$ (1.6 ± 0.0 g mol^{-1}) therein demonstrated that Fe likely contributed to increase the N-conversion efficiency during Chl a generation (Twining & Baines, 2015). In addition, the values of $NCEI_{N+P}$ and $NCEI_{N+P+Fe}$ were generally higher than those of $NCEI_N$ at S1, S2, S3, and S4 (Fig. 6), indicative of the fact that added P contributed to the increased N utilization efficiency at these stations. Indeed, P is an important part of the ribosome and can promote cell division (Arrigo, 2005), which likely increased the NCEI values to some extent. Liu et al. (2013) also reported the excessive P relative to N (N:P<16) in incubated seawater could increase the biomass. There were no significant differences in the NCEI values between the various treatments at S5, demonstrating that the effects of other nutrients (i.e., P and Fe) on N-conversion efficiency were negligible compared with N.

The NCEI in the AM-dust treatments was 1.3 ± 0.1 g mol^{-1} at S1 and 1.4 ± 0.6 g mol^{-1} at S4, which was 1.7- and 16.8-fold higher than those in the N treatments, respectively. (Fig. 6). Considering the P-limiting conditions at both stations, we concluded that the external supply of P associated with the AM-dust input likely also played a role in increasing the NCEI. Moreover, the $NCEI_{AM-dust}$ of 2.4 ± 0.1 g mol^{-1} was higher than $NCEI_{N+P+Fe}$ (1.8 ± 0.0 g mol^{-1}), $NCEI_{N+P}$ (1.6 ± 0.0 g mol^{-1}), and $NCEI_N$ (0.3 ± 0.2 g mol^{-1}) at S2. Apart from N, P, and Fe, AM-dust also provided considerable other nutrients, e.g., Mn and Co

360 (Table. 3), which may also have contributed to the phytoplankton growth in the incubations at S2 (Coale, 1991; Jakuba et al., 2008; Saito et al., 2008; Sunda, 2012). This potential synergistic effect is worthy of further investigation. At S3 and S5, the NCEI in AM-dust treatments, i.e., 1.2 ± 0.1 g mol^{-1} at S3, 1.1 ± 0.5 g mol^{-1} at S5, were similar to those in N treatments, i.e., 1.1 ± 0.1 g mol^{-1} at S3, 1.2 ± 0.2 g mol^{-1} at S5 (Fig. 6), indicating a negligible effect of the dissolved P from AM-dust on NCEI.

365 In recent years, more studies challenged to the use of 'Redfield ratio' to evaluate nutrient limiting conditions of phytoplankton (Klausmeier et al., 2004; Arrigo, 2005; Moore et al., 2013). Atmospheric aerosols characterized by mineral dust or anthropogenic pollutants contained complicated chemical components, their deposition to oceans can lead to complicated responses of phytoplankton (Guo et al., 2012; Paytan et al., 2009; Meng et al., 2016). The NCEI appears to have the advantage to reveal the possible mechanisms associated with the responses to some extents. For instance, phytoplankton at S1, S2, and 370 S3 were under co-limiting conditions of various nutrients, while the ratios of N:P in the seawaters were lower than 'Redfield ratio' of 16 (indicating N limitation). The difference of NCEI values among AM-dust and various nutrient treatments (N, P, N+P, N+P+Fe) allows quantifying the role of N, P, and Fe in stimulating phytoplankton growth (Fig. 6). Moreover, the NCEI also reveals other nutrients which may have a promotion effect on phytoplankton at S2. Note that the calculation of NCEI was based on the change of Chl a rather than biomass. In general, phytoplankton biomass increased with Chl a, which is an essential 375 component for photosynthesis. However, as C:Chl a ratios could vary for different phytoplankton assemblages (Sathyendranath et al., 2009), the relationship between biomass and N nutrients needs to be further investigated.

Fig. 7 shows the changes in the three size-fractionated Chl a concentrations in the treatments, relative to the corresponding controls. Generally, the relative changes in the size-fractionated Chl a in AM-dust treatments showed a decreasing trend with 380 decreasing cell size, i.e., micro- $\geqslant$ nano- $\geqslant$ pico-sized cells, consistent with the pattern observed in N+P+Fe treatments. Previous incubation experiments have also showed that addition of Asian aerosols could shift the phytoplankton size towards larger cells (Guo et al., 2012; Liu et al., 2013). Indeed, micro- and nano-sized cells, as indicated by faster uptake rates for nutrients and higher biomass-specific production rates, have a growth advantage relative to the pico-sized cells, when the added materials relieve the nutrient-limiting pressures (Cermeno et al., 2005; Maranon et al., 2007&2012). Besides, the relative

changes in micro- and nano-sized Chl *a* in AM-dust treatments were generally higher than in the N treatments at S1, S2, and S4. Especially for station S2, the relative changes in micro- and nano-sized Chl *a* in the AM-dust treatments were even larger than in the N+P treatments, and comparable to those in the N+P+Fe treatments (Fig. 7). These results demonstrated the importance of increased bioavailability of P at S1 and S4, and that of P and Fe at S2, following AM-dust addition, which supported the growth of micro- and nano-sized phytoplankton.

When the cell abundances of large-sized phytoplankton were considered, we also found that the addition of AM-dust induced larger increases than N additions after certain incubation days at S1 and S2, as characterized by co-limitation of multiple nutrients. Especially at S2, the increase in large phytoplankton abundance was even larger than in the N+P treatments and lower than in the N+P+Fe treatments. However, for station S3, characterized by NP co-limitation, the changes in the cell abundance of large-sized phytoplankton in AM-dust treatments were comparable to those in the N treatments. These results indicated that the supply of NP and NPFe induced by AM-dust addition, likely contributed to the increase in large-sized cell abundance at S1 and S2, respectively, whereas the supplied N from AM-dust likely determined the growth of large-sized phytoplankton at S3, because the supply of P from the AM-dust was negligible relative to the baseline P stocks (~0.11 μmol L^{-1}). For station S5, characterized by N limitation alone, the addition of AM-dust provided the limiting nutrient to increase the cell abundance of large-sized phytoplankton (Fig. 5).

Diatoms generally dominated the phytoplankton community in the control and treatments during the successive increase in the incubation period at S1, S2, S3, and S5 (Fig. 5). The addition of AM-dust and limited nutrients induced a notable increase in the diatom cell abundance at the four stations. Indeed, when the nutrient-limitation stress were relieved, diatoms tended to prosper rapidly, which was ascribed to their fast uptake rates and quick metabolic responses to enhanced nutrient availability (Fawcett and Ward, et al., 2011; Franz et al., 2012). The dominant species of diatoms (*Chaetoceros* spp., *Nitzschia* spp. in the open ocean and *Thalassiosira* spp., *Skeletonema* spp., *Cylindrotheca closterium*, *Rhizosolenia setigera*, *Nitzschia* spp. in the YS) in this study were similar to those reported in the North Pacific and YS (Noiri et al., 2005; Aizawa et al., 2005; Sun et al., 2013). Although the dominated algae at S4 was diatoms in treatments that received various additions, a shift of community

structure from diatoms to dinoflagellates was observed for AM-dust and N additions relative to the control. The contributions

of dinoflagellates to the large-sized phytoplankton community in cell abundance reached 40%–48%, while there was only

18%–28% among the P, N+P, and N+P+Fe treatments (Fig. 5). This was closely related to the fast growth of diatoms as a result

of the relief from P-limiting conditions after the addition of P, N+P, and N+P+Fe. Besides, it has been reported that

dinoflagellates with lower demands and higher P absorption efficiency have an advantage of surviving in P-deficient conditions,

compared with diatoms (Egge, 1998; Zhou et al., 2008). Hence, in contrast to P-related treatments, the supply of bioavailable

P from AM-dust was not enough to support the growth of diatoms at S4 (Fig. 5).

4.3 Bioavailable P in the AM-dust addition experiment

The increase in bioavailable P concentration following AM-dust addition played an important role in stimulating phytoplankton

growth at S1, S2, and S4, as mentioned above (Sect. 4.2). However, we did not detect a marked increase in the PO_4^{3-}

concentrations in incubated seawaters, following AM-dust additions, during the successive increase in incubation period at the

three stations (Fig. 3). This could be ascribed to the gradual bioavailable P released over time and its rapid uptake by

phytoplankton with a high P demand (Mackey et al., 2012), and the easy adsorption of PO_4^{3-} by particles or bottle walls (Liu

et al., 2013), which likely increases of PO_4^{3-} concentration in the incubated seawaters below the detection limit. In order to

quantify the increased bioavailable P concentrations following AM-dust addition, we analysed the correlation of the $C_{N:P}$ and

$S_{N:P}$ in AM-dust and N treatments in Fig 8.

$C_{N:P}$ significantly increased with $S_{N:P}$ (Fig. 8), and the same trend was observed at each station (Fig. S2). Klausmeier et al.

(2004, 2008) pointed out that the phytoplankton in nutrient-rich environments tends to exhibit an exponential/bloomer growth

with a requirement of N:P ratio in a relatively constant value, regardless of the varying nutrient supply ratios. However, when

the phytoplankton tend to sustain a competitive equilibrium status in nutrient-limited environments, e.g., N or P, their

requirements of N:P ratios generally increase with the nutrient supply ratios. In our study, the phytoplankton at the five stations

were limited by different nutrients, and thus, tended to sustain a competitive equilibrium status. As the provided DIN following

the AM-dust addition was 1.15 μmol N L^{-1}, lower than the amount of N when added alone (2 μmol N L^{-1}), the $S_{N:P}$ in AM-dust treatment was lower than that in N treatments. Thus, $C_{N:P}$ in both treatments at each station would follow the pattern: $C_{N:P}$ in AM-dust treatments $\leqslant$ $C_{N:P}$ in N treatments. The consumed N in AM-dust treatments, as well as N and P in N treatments, can be determined on basis of nutrient measurements at the beginning and the end of the successive increase in the incubation period (Fig. 3).

Because of $C_{N:P}$ in AM-dust treatments $\leqslant$ $C_{N:P}$ in N treatments, an inquality can be obtained as below

$$CP_{AD} \geq \frac{CN_{AD} \times CP_N}{CN_N} \tag{2}$$

where CP and CN are the consumed bioavailable P and $NO_3^- + NO_2^-$ concentrations (μmol L^{-1}) in the incubation systems during the successive increase in incubation period, respectively. Subscript means AM-dust ('AD') or N treatments.

The calculated result of the right term can be considered as the lower limit of the consumed P in the AM-dust treatments. They were 76 nmol L^{-1} at S1, 46 nmol L^{-1} at S2, 98 nmol L^{-1} at S3, 122 nmol L^{-1} at S4, and 20 nmol L^{-1} at S5. Deducting the P concentrations in the baseline seawaters (Table 2), the minimum bioavailable P supplied by AM-dust additions were estimated to be 22 nmol L^{-1} at S1, -5 nmol L^{-1} at S2, -6 nmol L^{-1} at S3, 18 nmol L^{-1} at S4, and -20 nmol L^{-1} at S5. Note that the dissolved P from AM-dust was as low as 8.6 nmol L^{-1} in the incubation bottles, which could not meet demands of phytoplankton at S1 and S4. The negative values implied the P concentrations in baseline seawaters were likely enough to support the growth of phytoplankton.

Thus, the supply other than the theoretically dissolved bioavailable P of 8.6 nmol L^{-1} induced by the AM-dust might exist. As reported in literature, the dissolved organic phosphorus (DOP) is considered a significant portion of the dissolved P pool in oceans, especially in surface seawater (Paytan and McLaughlin, 2007). Dust input has been reported to induce the biological mineralization of DOP to DIP under P-deficient conditions, and consequently, increased P bioavailability. DIP mineralized from DOP in the seawater would even accumulate if the demand of phytoplankton for P was small (Mackey et al., 2012). Trace

elements such as Co is an important component of the metalloenzyme alkaline phosphatase, which could facilitate the acquisition of bioavailable P from the DOP pool (Cembella et al., 1982; Jakuba et al., 2008). The concentration of Co nutrient in the surface seawater of the North Pacific generally maintained at picomolar levels (Sunda, 2012; Biller and Bruland, 2012), and the supplied Co of ~90 pmol L^{-1} by AM-dust addition (Table 3) likely played a role in increasing P bioavailability in this study. Note that the gradual enhanced solubility of atmospheric P with the duration of exposure in seawater was also reported to contribute additional bioavailable P for phytoplankton growth (Ridame and Guieu, 2002; Mackey et al., 2012). Unfortunately, no measurements of trace metal concentrations in seawaters as well as DOP and P contents in the phytoplankton cells were available in our study. The lack of data increased the uncertainty in data interpretation, which needs to be substantiated in a future study.

5 Conclusion

In this study, phytoplankton growth was found to be limited by two or more nutrients (i.e., NP or NPFe) in the NWPO, and by a single nutrient (i.e., N or P) in the YS. In the subtropical gyre of the NWPO, the addition of AM-dust provided NP or NPFe and micro-constituents to stimulate phytoplankton growth. In comparison with the controls, the maximum Chl *a* following AM-dust addition showed a 1.7- and 2.8-fold increase, while the cell abundance of large-sized phytoplankton showed a 1.8- and 3.9-fold increase. As the increased P from AM-dust was negligible in comparison with the baseline P stocks, the dissolved N from AM-dust, thus, primarily supported the phytoplankton growth in the *Kuroshio* extension. The maximum Chl *a* concentrations and cell abundance of large-sized phytoplankton following AM-dust addition were 1.3-fold and 1.7-fold larger, respectively, than those in the controls. In the YS, the increased P or N by AM-dust additions primarily contributed to the growth of phytoplankton. The Chl *a* concentrations in AM-dust treatments were generally higher than those in the controls, although the differences in maximum Chl *a* were negligible in both groups. The increase in the cell abundance of large-sized phytoplankton was < 1.7-fold, compared with the controls. Comparing the difference in consumed N:P between the AM-dust and N treatments, we found that the directly supplied bioavailable P by AM-dust in the incubated seawaters was not enough to support phytoplankton growth in the YS, which is characterized by P limitation, and in the subtropical gyre, which is

characterized by NP co-limitation. This suggests that there are other sources of P in the incubations, which may be explained by the enhanced solubility of P from AM-dust and/or mineralization of DOP in the seawaters. Besides, the addition of AM-dust had a potential to shift the phytoplankton towards larger cells at all incubation stations, although it did not change the dominant taxa of phytoplankton assemblages. In general, larger positive responses of phytoplankton induced by combined nutrients than by single nutrient from the AM-dust were observed in our study. This is likely related to the varying nutrient levels, community structures of phytoplankton in the baseline seawaters, and the input of nutrients following AM-dust addition.

Our study proposes the importance of increase in bioavailable P stock for phytoplankton growth following AM-dust addition. This would help us better understand the effects of dust deposition on P cycles in the ocean. In view of the increasing anthropogenic N deposition in the NWPO and YS, due to continuously strong NO_x emissions in the eastern Asia (Kim et al., 2011; Kim et al., 2014), the increase in bioavailable P stock induced by dust deposition might be even more important in phytoplankton growth in the future. Moreover, further investigations are needed to better understand the differential effects of increase in bioavailable P stock as a result of the atmospheric deposition on phytoplankton growth in the coastal seas and open oceans. In terms of autotrophs, the stimulation of large-sized phytoplankton growth due to the input of AM-dust might enhance the carbon storage in the deep ocean, as the sinking rate of large-sized cells in the water column are higher than the pico-sized ones (Bach et al., 2012). On the other hand, the increasing anthropogenic activities in recent years can also increase the contents of heavy metal in the dust, which may inhibit phytoplankton growth (Miao et al., 2005; Paytan et al., 2009). However, the toxic effect of dust aerosol was not well reflected in our study. Therefore, further studies are also needed to illustrate the two-blade function of dust deposition to the marine ecosystems.

Acknowledgments. This work was funded by National Natural Science Foundation of China (NSFC) (41210008: Gao), Major State Basic Research Development Program of China (973 Program) (2014CB953701: Gao), and NSFC and Royal Society travel grant (4141101141: Gao and Shi).

References

Arrigo, K. R.: Marine microorganisms and global nutrient cycles, Nature, 437, 349-355, doi: 10.1038/nature04158, 2005.

Aizawa, C., Tanimoto, M., and Jordan, R. W: Living diatom assemblages from North Pacific and Bering Sea surface waters during summer 1999. Deep Sea Research Part II: Topical Studies in Oceanography, 52, 2186-2205, doi: 10.1016/j.dsr2.2005.08.008, 2005.

Bach, L. T., Riebesell, U., Sett, S., Febiri, S., Rzepka, P., and Schulz, K. G.: An approach for particle sinking velocity measurements in the 3–400 μm size range and considerations on the effect of temperature on sinking rates, Marine biology, 159, 1853-1864, doi: 10.1007/s00227-012-1945-2, 2012.

Baker, A., Kelly, S., Biswas, K., Witt, M., and Jickells, T.: Atmospheric deposition of nutrients to the Atlantic Ocean, Geophysical Research Letters, 30, 2296, doi: 10.1029/2003GL018518, 2003.

Biller, D. V., and Kenneth W. B.: Analysis of Mn, Fe, Co, Ni, Cu, Zn, Cd, and Pb in seawater using the Nobias-chelate PA1 resin and magnetic sector inductively coupled plasma mass spectrometry (ICP-MS), Marine Chemistry, 130, 12-20, doi: 10.1016/j.marchem.2011.12.001, 2012.

Boyd, P. W., Jickells, T., Law, C., Blain, S., Boyle, E., Buesseler, K., Coale, K., Cullen, J., De Baar, H., and Follows, M.: Mesoscale iron enrichment experiments 1993-2005: Synthesis and future directions, science, 315, 612-617, doi: 10.1126/science.1131669, 2007.

Brown, M. T., Landing, W. M., and Measures, C. I.: Dissolved and particulate Fe in the western and central North Pacific: Results from the 2002 IOC cruise, Geochemistry, Geophysics, Geosystems, 61, 1-20, doi: 10.1029/2004GC000893, 2005.

Burson, A., Stomp, M., Akil, L., Brussaard, C. P., and Huisman, J.: Unbalanced reduction of nutrient loads has created an offshore gradient from phosphorus to nitrogen limitation in the North Sea, Limnology and Oceanography, 61, 869-888, doi: 10.1002/lno.10257, 2016.

Cembella, A. D., Antia, N. J., and Harrison, P. J.: The utilization of inorganic and organic phosphorous compounds as nutrients by eukaryotic microalgae: A multidisciplinary perspective: Part I, CRC Critical Reviews in Microbiology, 10, 317-391, doi: 10.3109/10408418209113567, 1982.

530 Cermeno, P., Estevez-Blanco, P., Maranón, E., and Fernandez, E.: Maximum photosynthetic efficiency of size-fractionated phytoplankton assessed by ^{14}C uptake and fast repetition rate fluorometry, Limnology and Oceanography, 50, 1438-1446, doi:10.4319/lo.2005.50.5.1438, 2005.

Chien, C. T., Mackey, K. R., Dutkiewicz, S., Mahowald, N. M., Prospero, J. M., and Paytan, A.: Effects of African dust deposition on phytoplankton in the western tropical Atlantic Ocean off Barbados, Global Biogeochemical Cycles, 30, 716-734,
535 doi: 10.1002/2015GB005334, 2016.

Coale, K. H.: Effects of iron, manganese, copper, and zinc enrichments on productivity and biomass in the subarctic Pacific, Limnology and Oceanography, 36, 1851-1864, doi: 10.4319/lo.1991.36.8. 1851, 1991.

Coelho, F., Santos, A., Coimbra, J., Almeida, A., Cunha, A., Cleary, D., Calado, R., and Gomes, N.: Interactive effects of global climate change and pollution on marine microbes: the way ahead. Ecology and evolution, 3, 1808-1818, doi:
540 10.1002/ece3.565, 2013.

Egge, J. K: Are diatoms poor competitors at low phosphate concentrations?. Journal of Marine Systems, 16, 191-198, doi: 10.1016/S0924-7963(97)00113-9, 1998.

Duce, R., Liss, P., Merrill, J., Atlas, E., Buat-Menard, P., Hicks, B., Miller, J., Prospero, J., Arimoto, R., and Church, T.: The atmospheric input of trace species to the world ocean, Global biogeochemical cycles, 5, 193-259, doi: 10.1029/91GB01778,
545 1991.

Franz, J., Krahmann, G., Lavik, G., Grasse, P., Dittmar, T., and Riebesell, U: Dynamics and stoichiometry of nutrients and phytoplankton in waters influenced by the oxygen minimum zone in the eastern tropical Pacific. Deep Sea Research Part I: Oceanographic Research Papers, 62, 20-31, doi: 10.1016/j.dsr.2011.12.004, 2012.

Fawcett, S. E., and Ward, B. B.: Phytoplankton succession and nitrogen utilization during the development of an upwelling
550 bloom. Marine Ecology Progress Series, 428, 13-31, doi: 10.3354/meps09070, 2011.

Fu, M., Wang, Z., Li, Y., Li, R., Sun, P., Wei, X., Lin, X., and Guo, J.: Phytoplankton biomass size structure and its regulation in the Southern Yellow Sea (China): Seasonal variability. Continental Shelf Research, 29, 2178-2194, doi: 10.1016/j.csr.2009.08.010, 2009.

Formenti, P., S., L., Balkanski, Y., Desboeufs, K., Ebert, M., Kandler, A. Petzold, D. Scheuvens, S. Weinbruch, and Zhang, D.:

555   Recent progress in understanding physical and chemical properties of African and Asian mineral dust. Atmospheric Chemistry and Physics, 11, 8231-8256, doi: 10.5194/acp-11-8231-2011, 2011.

Gao, Y., Arimoto, R., Duce, R., Lee, D., and Zhou, M.: Input of atmospheric trace elements and mineral matter to the Yellow Sea during the spring of a low-dust year, Journal of Geophysical Research: Atmospheres, 97, 3767-3777, doi: 10.1029/91JD02686, 1992.

560   Grasshoff, K., Kremling, K., and Ehrhardt, M.: Methods of seawater analysis, 3 edn., Wiley-VCH, 1999.

Guieu, C., Dulac, F., Desboeufs, K., Wagener, T., Pulido-Villena, E., Grisoni, J.-M., Louis, F., Ridame, C., Blain, S., and Brunet, C.: Large clean mesocosms and simulated dust deposition: a new methodology to investigate responses of marine oligotrophic ecosystems to atmospheric inputs, Biogeosciences, 7, 2765-2784, doi: 10.5194/bg-7-2765-2010, 2010.

Guo, C., Yu, J., Ho, T.-Y., Wang, L., Song, S., Kong, L., and Liu, H.: Dynamics of phytoplankton community structure in the
565   South China Sea in response to the East Asian aerosol input, Biogeosciences, 9, 1519-1536, doi: 10.5194/bg-9-1519-2012, 2012.

Guo, X., Zhu, X., Wu, Q., and Huang, D.: The Kuroshio nutrient stream and its temporal variation in the East China Sea. Journal of Geophysical Research: Oceans, 117, C01026, doi: 10.1029/2011JC007292, 2012.

Hashihama, F., Furuya, K., Kitajima, S., Takeda, S., Takemura, T., and Kanda, J.: Macro-scale exhaustion of surface phosphate
570   by dinitrogen fixation in the western North Pacific, Geophysical Research Letters, 36, 3610, doi: 10.1029/2008GL036866, 2009.

Herut, B., Zohary, T., Krom, M., Mantoura, R., Pitta, P., Psarra, S., Rassoulzadegan, F., Tanaka, T., and Thingstad, T.: Response of East Mediterranean surface water to Saharan dust: On-board microcosm experiment and field observations. Deep Sea Research Part II: Topical Studies in Oceanography, 52, 3024-3040, doi: 10.1016/j.dsr2.2005.09.003, 2005.

575   Herut, B., Rahav, E., Tsagaraki, T., Giannakourou, A., Tsiola, A., Psarra, S., Lagaria, A., Papageorgiou, N., Mihalopoulos, N., and Theodosi, C.: The potential impact of Saharan dust and polluted aerosols on microbial populations in the East Mediterranean Sea, an overview of a mesocosm experimental approach, Frontiers in Marine Science, 3, 226, doi: 10.3389/fmars.2016.00226, 2016.

Hsu, S. C., Liu, S. C., Arimoto, R., Shiah, F. K., Gong, G. C., Huang, Y. T., Kao, S. J., Chen, J. P., Lin, F. J., and Lin, C. Y.:

580   Effects of acidic processing, transport history, and dust and sea salt loadings on the dissolution of iron from Asian dust, Journal of Geophysical Research: Atmospheres, 115, 1485-1490, doi: 10.1029/2009JD013442, 2010.

Jakuba, R. W., Moffett, J. W., and Dyhrman, S. T.: Evidence for the linked biogeochemical cycling of zinc, cobalt, and phosphorus in the western North Atlantic Ocean, Global Biogeochemical Cycles, 22, 1971-1976, doi: 10.1029/2007GB003119, 2008.

585   Jickells, T., An, Z., Andersen, K. K., Baker, A., Bergametti, G., Brooks, N., Cao, J., Boyd, P., Duce, R., and Hunter, K.: Global iron connections between desert dust, ocean biogeochemistry, and climate, science, 308, 67-71, doi: 10.1126/science.1105959, 2005.

Kanakidou, M., Duce, R. A., Prospero, J. M., Baker, A. R., Benitez-Nelson, C., Dentener, F. J., Hunter, K. A., Liss, P. S., Mahowald, N., and Okin, G. S.: Atmospheric fluxes of organic N and P to the global ocean, Global Biogeochemical Cycles,

590   26, GB3026, doi: 10.1029/2011GB004277, 2012.

Kim, I.-N., Lee, K., Gruber, N., Karl, D. M., Bullister, J. L., Yang, S., and Kim, T.-W.: Increasing anthropogenic nitrogen in the North Pacific Ocean, Science, 346, 1102-1106, doi: 10.1126/science.1258396, 2014.

Kim, T. W., Lee, K., Najjar, R. G., Jeong, H. D., and Jeong, H. J.: Increasing N abundance in the northwestern Pacific Ocean due to atmospheric nitrogen deposition. Science, 334, 505-509, doi: 10.1126/science.1206583, 2011.

595   Kitajima, S., Furuya, K., Hashihama, F., Takeda, S., and Kanda, J.: Latitudinal distribution of diazotrophs and their nitrogen fixation in the tropical and subtropical western North Pacific, Limnology and Oceanography, 54, 537-547, doi: 10.4319/lo.2009.54.2.0537, 2009.

Klausmeier, C. A., Litchman, E., Daufresne, T., and Levin, S. A.: Optimal nitrogen-to-phosphorus stoichiometry of phytoplankton, Nature, 429, 171-174, doi: 10.1038/nature02454, 2004.

600   Klausmeier, C. A., Litchman, E., and Levin, S. A.: Phytoplankton growth and stoichiometry under multiple nutrient limitation. Limnology and Oceanography, 49, 1463-1470, doi: 10.4319/lo.2004.49.4_part_ 2.1463, 2004.

Klausmeier, C. A., Litchman, E., Daufresne, T., and Levin, S.: Phytoplankton stoichiometry, Ecological Research, 23, 479-485, doi: 10.1007/s11284-008-0470-8, 2008.

Krom, M. D., Shi, Z., Stockdale, A., Berman-Frank, I., Giannakourou, A., Herut, B., Lagaria, A., Papageorgiou, N., Pitta, P.,

and Psarra, S.: Response of the Eastern Mediterranean microbial ecosystem to dust and dust affected by acid processing in the atmosphere, Frontiers in Marine Science, 3, 133, doi: 10.3389/fmars.2016.00133, 2016.

Li, Q., Legendre, L., and Jiao, N.: Phytoplankton responses to nitrogen and iron limitation in the tropical and subtropical Pacific Ocean, Journal of Plankton Research, 37, 306–319, doi: 10.1093/plankt/fbv008, 2015.

Liu, S., Zhang, J., Chen, S. Z., Chen, H., Hong, G., Wei, H., and Wu, Q.: Inventory of nutrient compounds in the Yellow Sea, Continental Shelf Research, 23, 1161-1174, doi: 10.1016/S0278-4343(03)00089-X, 2003.

Liu, Y., Zhang, T., Shi, J., Gao, H., and Yao, X.: Responses of chlorophyll a to added nutrients, Asian dust, and rainwater in an oligotrophic zone of the Yellow Sea: Implications for promotion and inhibition effects in an incubation experiment, Journal of Geophysical Research: Biogeosciences, 118, 1763-1772, doi: 10.1002/2013JG002329, 2013.

Mackey, K. R., Roberts, K., Lomas, M. W., Saito, M. A., Post, A. F., and Paytan, A.: Enhanced solubility and ecological impact of atmospheric phosphorus deposition upon extended seawater exposure, Environmental science & technology, 46, 10438-10446, doi: 10.1021/es3007996, 2012.

Maranon, E., Cermeno, P., Rodríguez, J., Zubkov, M. V., and Harris, R. P.: Scaling of phytoplankton photosynthesis and cell size in the ocean, Limnology and oceanography, 52, 2190-2198, doi: 10.2307/4502368, 2007.

Maranon, E., Fernandez, A., Mourino-Carballido, B., Martinez-Garcia, S., Teira, E., Cermeno, P., Choucino, P., Huete-Ortega, M., Fernandez, E., Calvo-Diaz, A., Anxelu, X., Moran, G., Bode, A., Moreno-Ostos, E., Varela, M. M., Patey, M. D., and Achterberg, E. P: Degree of oligotrophy controls the response of microbial plankton to Saharan dust, Limnology and Oceanography, 55, 2339-2352, doi: 10.4319/lo.2010.55.6.2339, 2010.

Maranon, E., Cermeno, P., Latasa, M., and Tadonleke, R. D.: Temperature, resources, and phytoplankton size structure in the ocean, Limnology and Oceanography, 57, 1266-1278, doi: 10.4319/lo.2012.57.5.1266, 2012.

Martin, J. H.: Iron still comes from above, Nature, 353, 123-123, doi: 10.1038/353123b0, 1991.

Measures, C., Cutter, G., Landing, W., and Powell, R.: Hydrographic observations during the 2002 IOC Contaminant Baseline Survey in the western Pacific Ocean, Geochemistry, Geophysics, Geosystems, 7, Q03M06, doi: 10.1029/2004GC000855, 2006.

Meng, X., Chen, Y., Wang, B., Ma, Q., and Wang, F.: Responses of phytoplankton community to the input of different aerosols in the East China Sea, Geophysical Research Letters, 43, 7081-7088, doi: 10.1002/2016GL069068, 2016.

630 Miao, A., Wang, W., and Philippe, J.: Comparison of Cd, Cu, and Zn toxic effects on four marine phytoplankton by pulse-amplitude-modulated fluorometry. Environmental Toxicology & Chemistry, 24(10), 2603-2611, doi: 10.1897/05-009R.1, 2005.

Mills, M. M., Ridame, C., Davey, M., La Roche, J., and Geider, R. J.: Iron and phosphorus co-limit nitrogen fixation in the eastern tropical North Atlantic, Nature, 429, 292-294, doi: 10.1038/nature02550, 2004.

Moore, C., Mills, M., Arrigo, K., Berman-Frank, I., Bopp, L., Boyd, P., Galbraith, E., Geider, R. J., Guieu, C., and Jaccard, S.:

635 Processes and patterns of oceanic nutrient limitation, Nature Geoscience, 6, 701-710, doi: 10.1038/NGEO1765, 2013.

Moore, C. M., Mills, M. M., Langlois, R., Milne, A., Achterberg, E. P., LaRoche, J., and Geider, R. J.: Relative influence of nitrogen and phosphorous availability on phytoplankton physiology and productivity in the oligotrophic sub-tropical North Atlantic Ocean, Limnology and Oceanography, 53, 291-305, doi: 10.4319/lo.2008.53.1.0291, 2008.

Noiri, Y., Kudo, I., Kiyosawa, H., Nishioka, J., and Tsuda, A.: Influence of iron and temperature on growth, nutrient utilization

640 ratios and phytoplankton species composition in the western subarctic Pacific Ocean during the SEEDS experiment, Progress in Oceanography, 64, 149-166, doi: 10.1016/j.pocean.2005.02.006, 2005.

Nishibe, Y., Takahashi, K., Shiozaki, T., Kakehi, S., Saito, H., and Furuya, K.: Size-fractionated primary production in the Kuroshio Extension and adjacent regions in spring. Journal of oceanography, 71, 27-40, doi:10.1007/s10872-014-0258-0, 2015.

Ooki, A., and Uematsu, M.: Chemical interactions between mineral dust particles and acid gases during Asian dust events,

645 Journal of Geophysical Research: Atmospheres, 110, 1447-1454, doi: 10.1029/2004JD004737, 2005.

Paytan, A., and McLaughlin, K.: The oceanic phosphorus cycle, Chemical reviews, 107, 563-576, doi: 10.1021/cr0503613, 2007.

Paytan, A., Mackey, K. R., Chen, Y., Lima, I. D., Doney, S. C., Mahowald, N., Labiosa, R., and Post, A. F.: Toxicity of atmospheric aerosols on marine phytoplankton. Proceedings of the National Academy of Sciences, 106(12), 4601-4605, doi:

650 10.1073/pnas.0811486106, 2009.

Ridame, C., and Guieu, C.: Saharan input of phosphate to the oligotrophic water of the open western Mediterranean Sea, Limnology and Oceanography, 47, 856-869, doi:10.4319/lo.2002.47.3.0856, 2002.

Ridame, C., Dekaezemacker, J., Guieu, C., Bonnet, S., L'Helguen, S., and Malien, F.: Contrasted Saharan dust events in LNLC environments: impact on nutrient dynamics and primary production, Biogeosciences, 11, 4783-4800, doi: 10.5194/bg-11-4783-

655 2014, 2014.

Saito, M. A., Goepfert, T. J., and Ritt, J. T.: Some thoughts on the concept of colimitation: three definitions and the importance of bioavailability, Limnology and Oceanography, 53, 276-290, doi: 10.2307/40006168, 2008.

Sathyendranath, S., Stuart, V., Nair, A., Oka, K., Nakane, T., Bouman, H., Forget, M. H., Maass, H., and Platt, T.: Carbon-to-chlorophyll ratio and growth rate of phytoplankton in the sea, Marine Ecology Progress Series, 383, 73-84, doi: 10.3354/meps07998, 2009.

660

Shao, Y., Wyrwoll, K.-H., Chappell, A., Huang, J., Lin, Z., McTainsh, G. H., Mikami, M., Tanaka, T. Y., Wang, X., and Yoon, S.: Dust cycle: An emerging core theme in Earth system science, Aeolian Research, 2, 181-204, doi: 10.1016/j.aeolia.2011.02.001, 2011.

Shi, J., Gao, H., Zhang, J., Tan, S., Ren, J., Liu, C., Liu, Y., and Yao, X.: Examination of causative link between a spring bloom and dry/wet deposition of Asian dust in the Yellow Sea, China, Journal of Geophysical Research: Atmospheres, 117, D17304, doi:10.1029/2012JD017983, 2012.

665

Shi, Z., Krom, M. D., Bonneville, S., Baker, A. R., Jickells, T. D., and Benning, L. G.: Formation of iron nanoparticles and increase in iron reactivity in mineral dust during simulated cloud processing, Environmental science & technology, 43, 6592-6596, doi: 10.1021/es901294g, 2009.

Strickland, J. D. H., and Parsons, T. R.: A practical handbook of seawater analysis, 1972.

670

Sunda, W.: Feedback interactions between trace metal nutrients and phytoplankton in the ocean, Frontiers in microbiology, 3, 204, doi: 10.3389/fmicb.2012.00204, 2012.

Sun, J., Feng, Y., Wang, D., Song, S., Jiang, Y., Ding, C., and Wu, Y.: Bottom-up control of phytoplankton growth in spring blooms in Central Yellow Sea, China. Deep Sea Research Part II: Topical Studies in Oceanography, 97, 61-71, doi: 10.1016/j.dsr2.2013.05.006, 2013.

675

Tanaka, T., Thingstad, T., Christaki, U., Colombet, J., Cornet-Barthaux, V., Courties, C., Grattepanche, J.-D., Lagaria, A., Nedoma, J., and Oriol, L.: Lack of P-limitation of phytoplankton and heterotrophic prokaryotes in surface waters of three anticyclonic eddies in the stratified Mediterranean Sea, Biogeosciences, 8, 525-538, doi:10.5194/bg-8-525-2011, 2011.

Twining, B. S. and Baines, S. B. The trace metal composition of marine phytoplankton. Annual review of marine science, 5,

680   191-215, doi: 10.1146/annurev-marine-121211-172322, 2013.

Wang, B. D., Wang, X. L., and Zhan, R. Nutrient conditions in the Yellow Sea and the East China Sea. Estuarine, Coastal and Shelf Science, 58, 127-136, doi: 10.1016/S0272-7714(03)00067-2, 2003.

Whitney, F. A.: Nutrient variability in the mixed layer of the subarctic Pacific Ocean, 1987–2010, Journal of Oceanography, 67, 481-492, doi: 10.1007/s10872-011-0051-2, 2011.

685   Yatsu, A., Chiba, S., Yamanaka, Y., Ito, S.-i., Shimizu, Y., Kaeriyama, M., and Watanabe, Y.: Climate forcing and the Kuroshio/Oyashio ecosystem, ICES Journal of Marine Science: Journal du Conseil, 70, 922-933, doi: 10.1093/icesjms/fst084, 2013.

Zhou, M. J., Shen, Z. L., and Yu, R. C.: Responses of a coastal phytoplankton community to increased nutrient input from the Changjiang (Yangtze) River. Continental Shelf Research, 28, 1483-1489, doi: 10.1016/j.csr.2007.02.009, 2008.

Table 1. Experimental information and baseline conditions at the sampling stations

	Ar4 (S1)	(G7) S2	K4 (S3)	B7 (S4)	H10 (S5)
Sampling date	2014.3.23	2014.4.5	2014.4.14	2014.5.9	2014.4.29
Incubation time	10 days	9 days	9 days	10 days	9 days
Sampling location	29.5°N, 142.5°E	30.0°N, 148.5°E	34.0°N, 144.0°E	37.00°N, 123.17°E	35.0°N, 124.0°E
Sea surface temperature (SST, °C)	18.9	18.3	18.6	9.8	12.6
Mixed layer depth (MLD, m)	150	82	103	-	18
Chl *a* (µg L^{-1})	0.24	0.50	1.28	1.58	2.74
NO$_3^-$+NO$_2^-$ (µmol L^{-1})	0.26	0.04	0.51	3.20	0.28
PO$_4^{3-}$ (µmol L^{-1})	0.05	0.05	0.11	0.10	0.04
N:P (µmol:µmol)	5	<1	5	32	7
Micro-sized Chl a (%)	6	8	28	14	27
Nano-sized Chl a (%)	18	19	23	36	37
Pico-sized Chl a (%)	76	73	49	50	36
Large-sized phytoplankton abundance (cell mL^{-1})	17	10	79	35	314
Diatoms (cell mL^{-1})	12	6	74	16	286
Dinoflagellates (cell mL^{-1})	5	4	5	19	28

Table 2. Treatments to the bioassay incubation experiments

Incubation No.	Treatments	Amended concentrations
1	Control	-
2	AM-dust	2 mg L^{-1}
3	$NaNO_3$	2 μmol L^{-1}
4	NaH_2PO_4	0.2 μmol L^{-1}
5*	$FeCl_3$	2 nmol L^{-1}
6	$NaNO_3$+NaH_2PO_4	2 μmol L^{-1}+0.2 μmol L^{-1}
7	$NaNO_3$+NaH_2PO_4+$FeCl_3$	2 μmol L^{-1}+0.2 μmol L^{-1}+2 nmol L^{-1}

*Only at stations S2 and S4.

Table 3. Nutrient and soluble trace-metal contents in artificially modified and untreated dust, and theoretically increased corresponding concentrations in the incubated seawaters amended with AM-dust.

	Nutrients (μmol g^{-1})				Soluble trace metals (μg g^{-1})						
	NO_3^-	NO_2^-	NH_4^+	PO_4^{3-}	Fe	Mn	Cu	Cd	Pb	Co	Zn
AM-dust	532.9	34.2	10.3	4.3	473.1	413.5	0.23	0.04	0.24	2.58	4.27
Untreated dust	133.2	8.6	10.5	1.3	22.7	1.66	ND[a]	ND	ND	ND	0.03
Increased concentrations amended with AM-dust (nmol L^{-1})[b]	1066	68.4	20.6	8.6	16.90	15.05	7.2E-3[c]	7.1E-4	2.3E-3	0.09	0.13

[a] 'ND' means no detection.

[b] Calculated by dividing the added amounts of nutrient and soluble trace metals with AM-dust input by the incubation volume of 20 L.

[c] 'E-number' indicates '$\times 10^{number}$'.
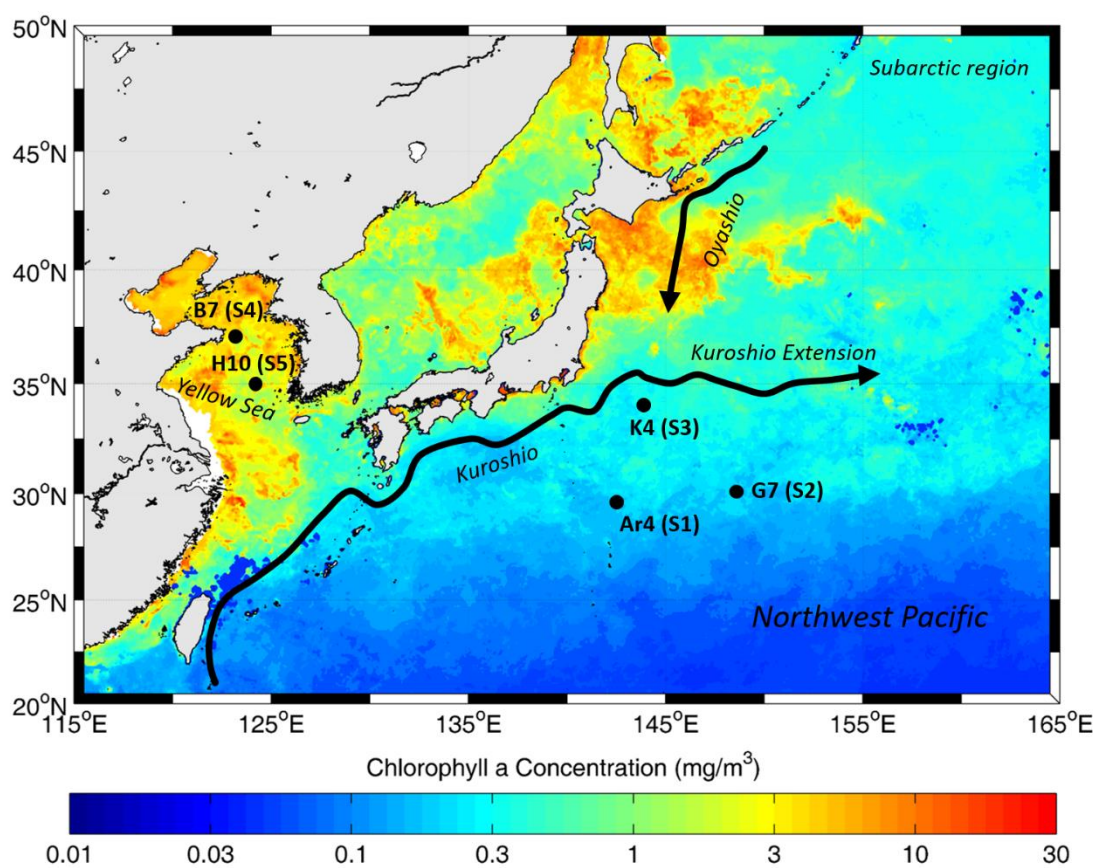
Figure 1. Locations of the five seawater-collection stations for the microcosm experiments (The base map reflects an average composite of Chl *a* concentrations in March-May, 2014 obtained from the NASA website (https://modis.gsfc.nasa.gov/data/dataprod/chlor_a.php)

710
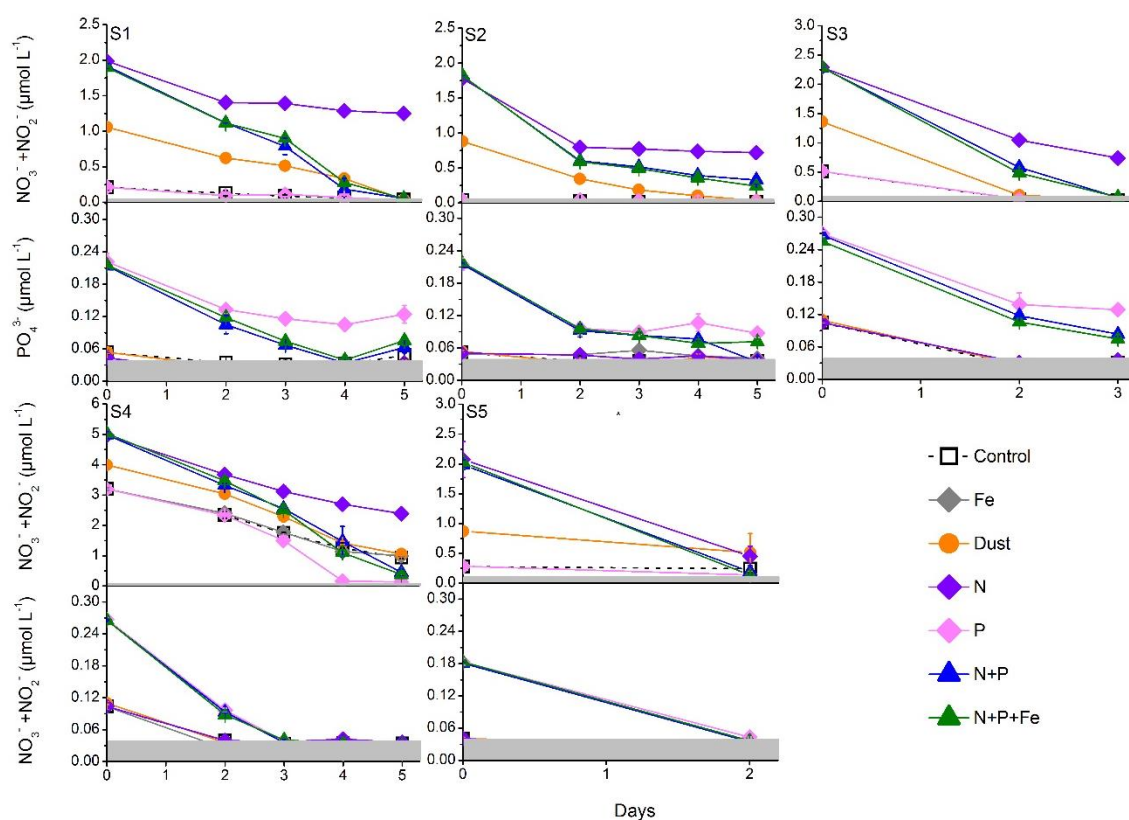
Figure 2. Changes in $NO_3^-+NO_2^-$ and PO_4^{3-} concentrations during the successive increase in the incubation period at each station. Shaded areas mean the values below the detection limit
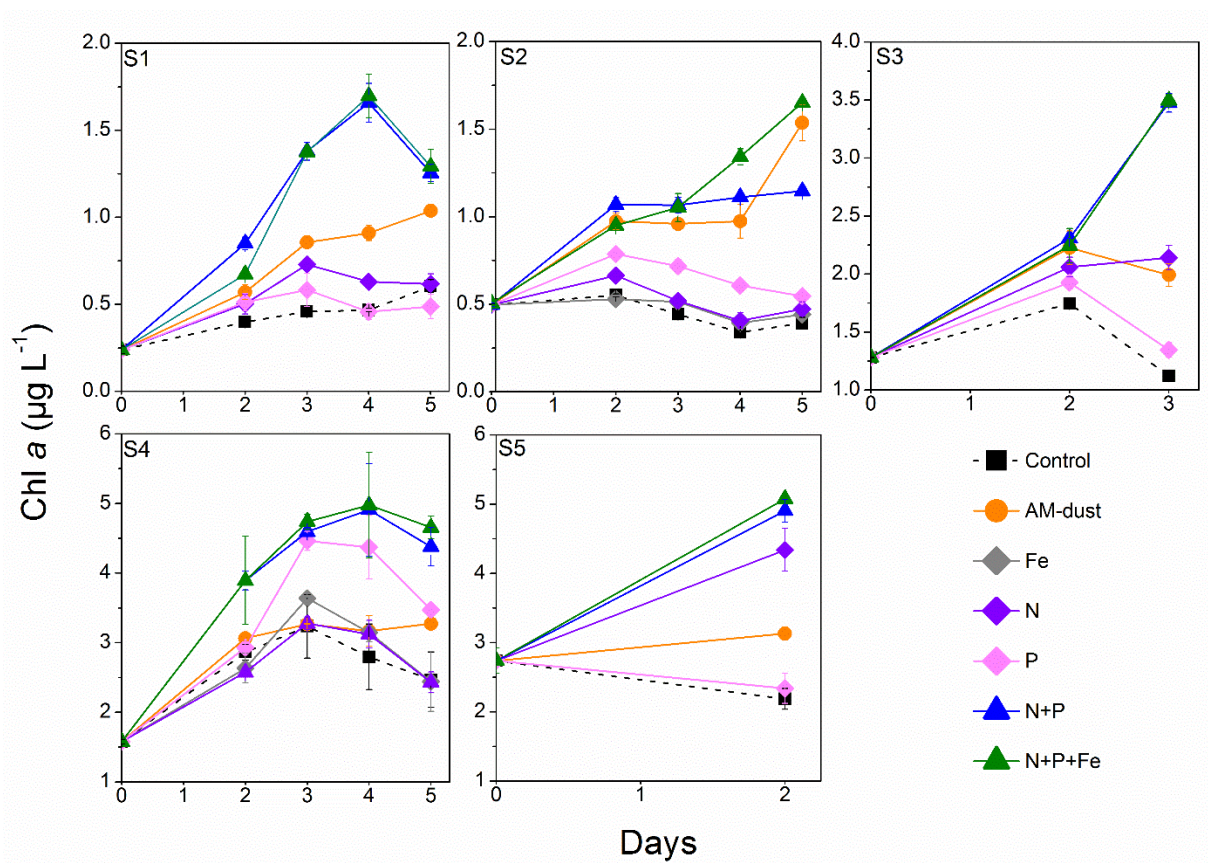
715 **Figure 3.** Changes in Chl *a* during the successive increase in the incubation period at each station
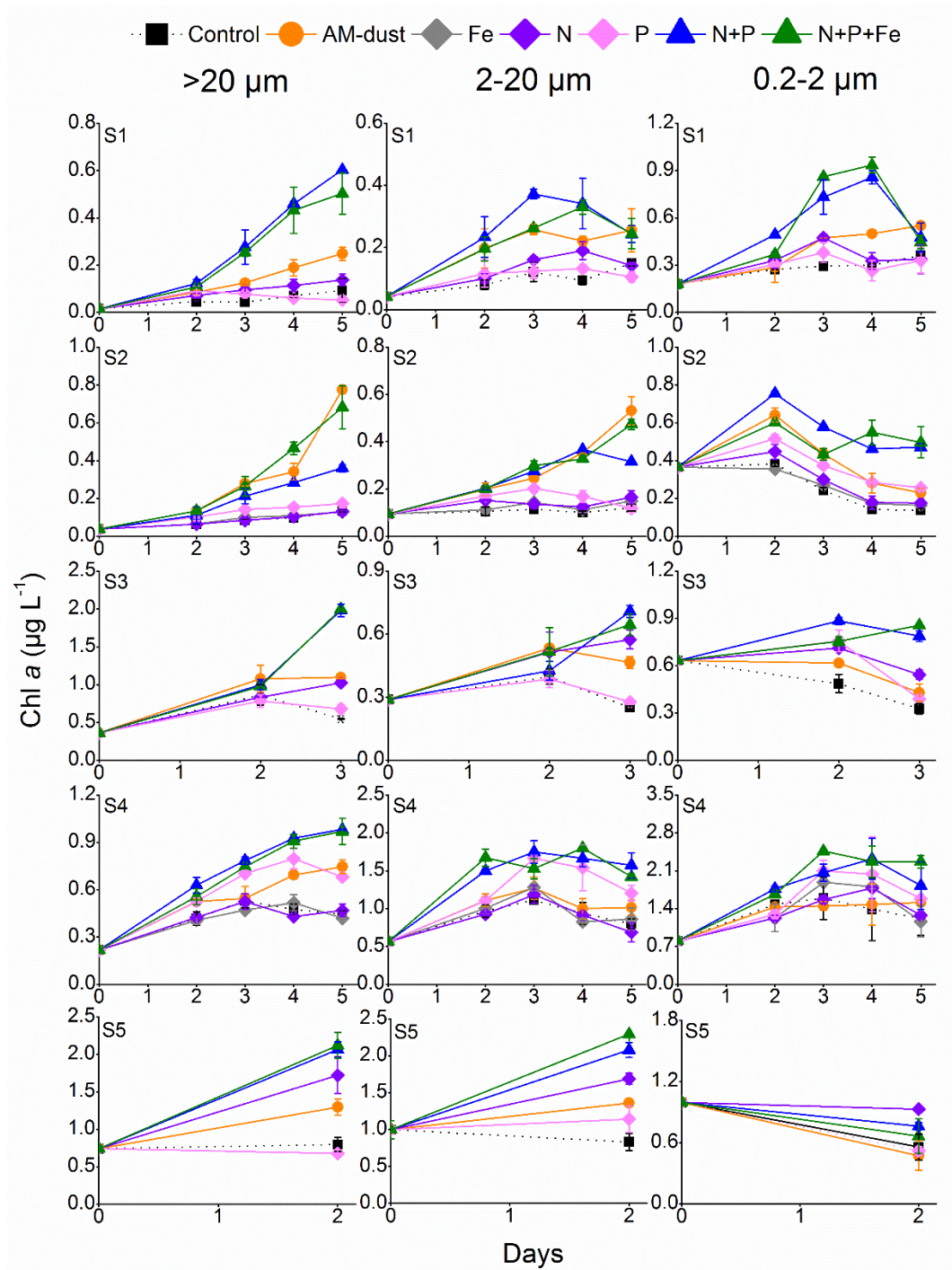
Figure 4. Changes in size-fractionated Chl *a* during the successive increase in the incubation period at each station

720
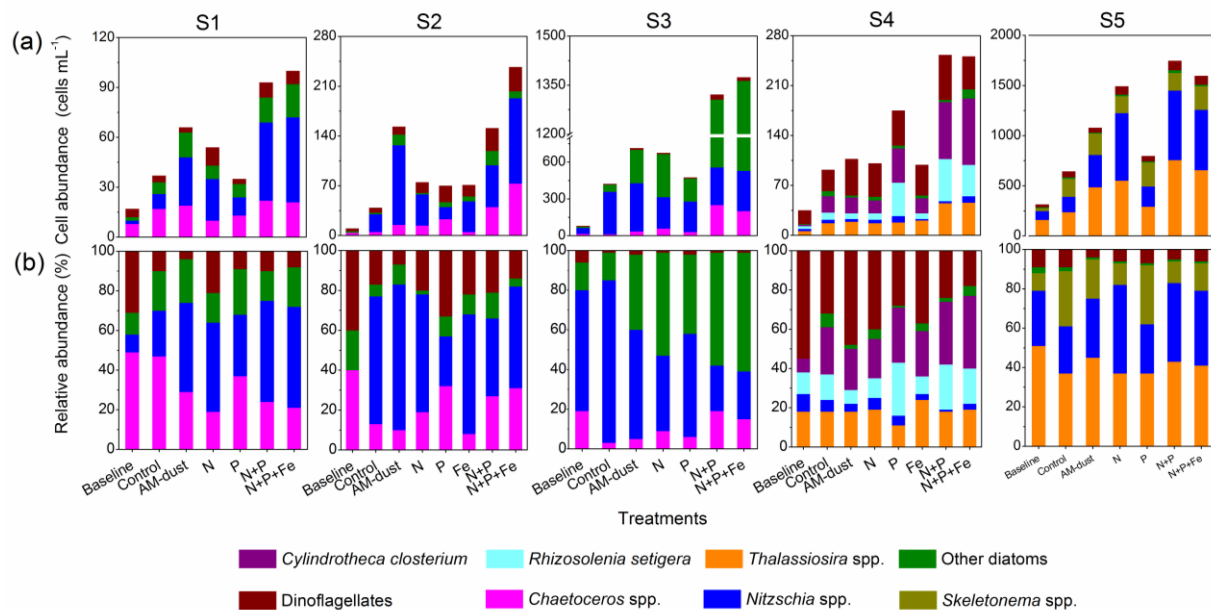
Figure 5. Changes in the taxonomic structure of large-sized phytoplankton community before (i.e., 'baseline') and during (i.e., 'control' and various treatments) the successive increase in the incubation period at each station. (a) Cell abundance of large-sized phytoplankton. (b) Relative abundance, i.e., the contribution of specific species to the large-sized phytoplankton community in cell abundance
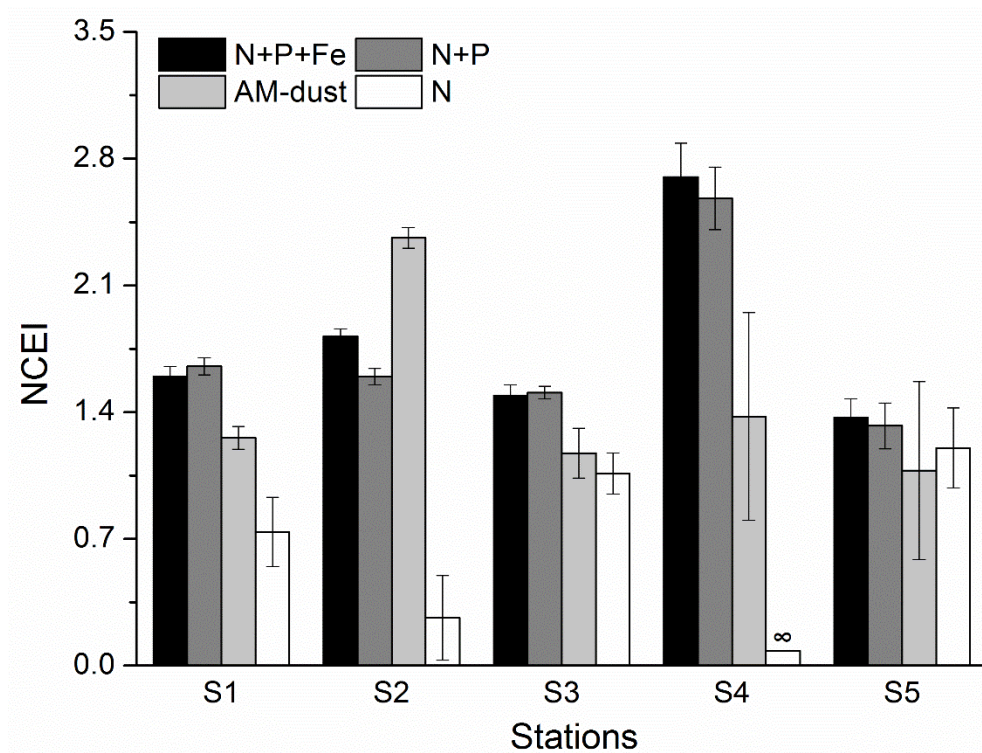
730 **Figure 6.** The net conversion efficiency index (NCEI) of N conversion to Chl *a* in AM-dust and various nutrient additions during the successive increase in the incubation period at each station. Error bars were calculated by propagating the standard deviation of NCEI in various treatments. "∞" indicates the standard deviation is at least threefold larger than the mean value of NCEI.

735
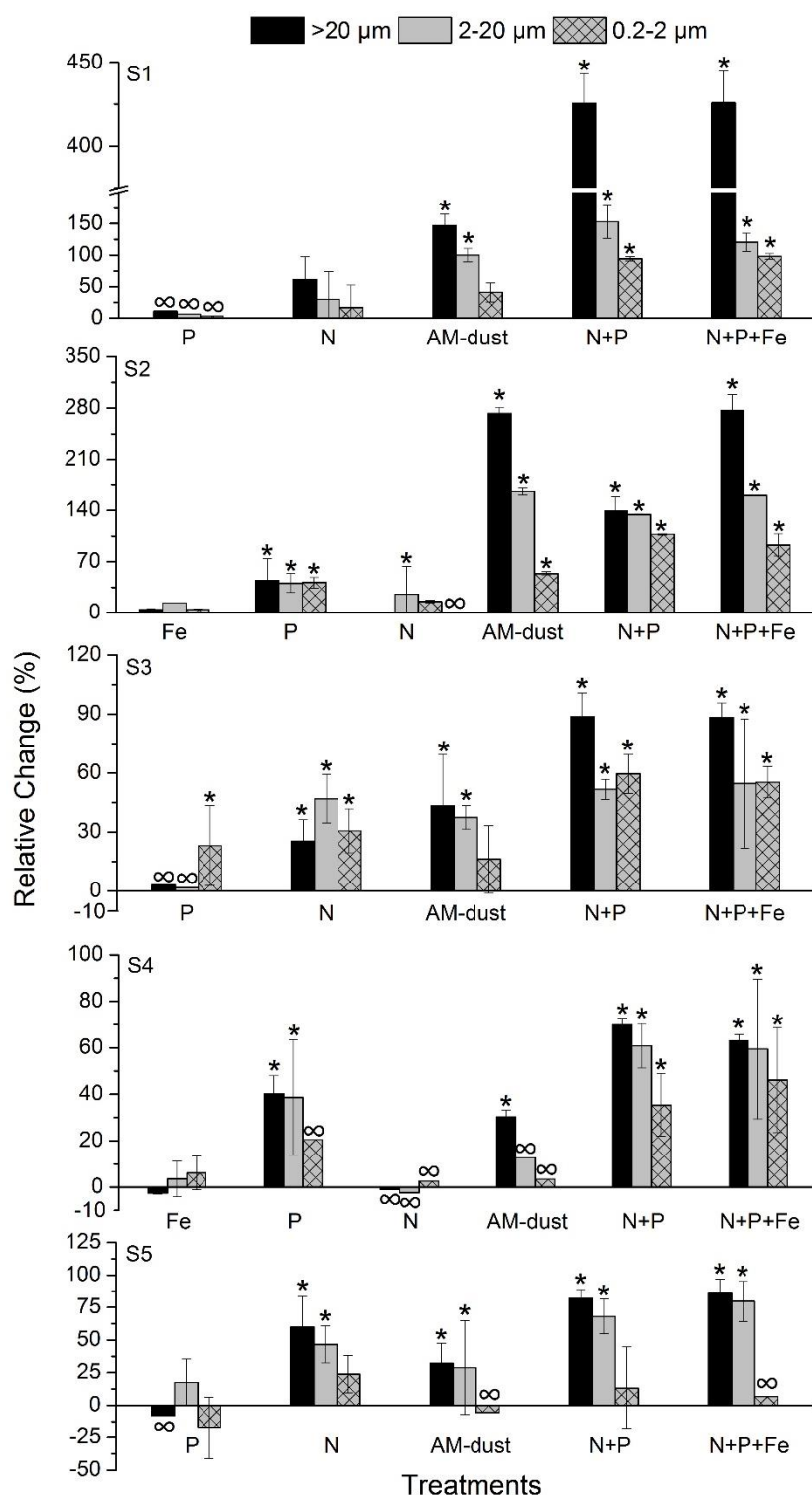
Figure 7. Relative change (%) in size-fractionated Chl *a* in AM-dust and various nutrient treatments during the successive increase in incubation period at each station. Relative change in this study was calculated as $100 \times ([\text{mean in treatments - mean in control}]/\text{mean in control})$. Error bars were calculated by propagating the standard deviation of mean values in the control and various treatments. "∞" indicates the standard deviation is at least threefold larger than the mean value of relative change. Asterisks indicate that the treatment induces a significant difference in the mean of Chl *a* compared with those in control ($p < 0.05$).
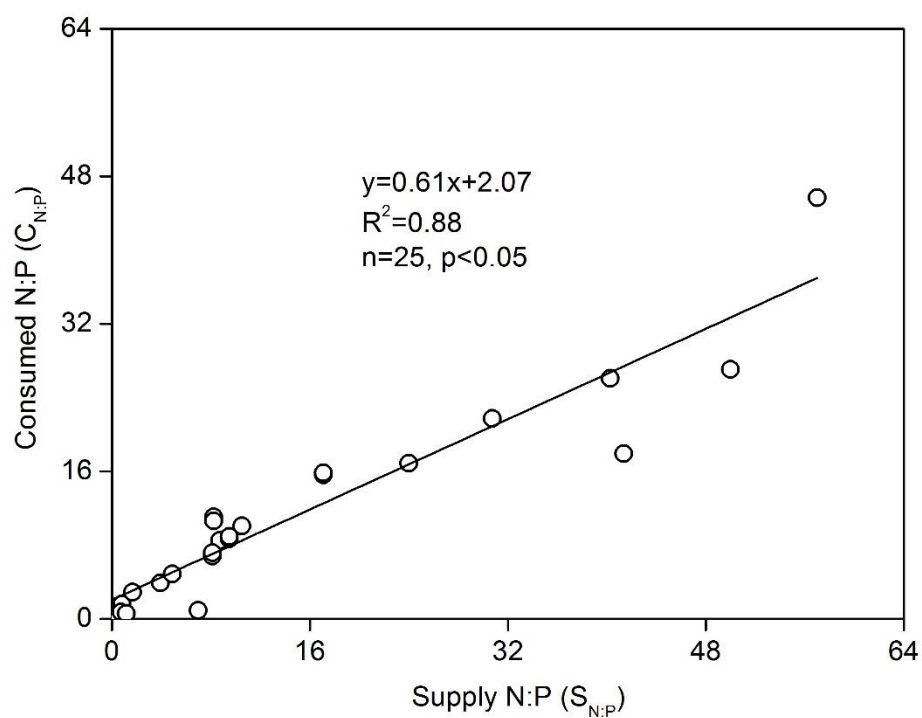
Figure 8. The relationship between the consumed N:P ratio ($C_{N:P}$) and supply N:P ratio ($S_{N:P}$) in the control and the various nutrient treatments during the successive increase in the incubation period at all stations.